



## Association between inflammation, reward processing, and ibuprofen-induced increases of miR-23b in astrocyte-enriched extracellular vesicles: A randomized, placebo-controlled, double-blind, exploratory trial in healthy individuals

Kaiping Burrows<sup>a,\*</sup>, Leandra K. Figueroa-Hall<sup>a,1</sup>, Ahlam M. Alarbi<sup>b,c</sup>, Jennifer L. Stewart<sup>a,d</sup>, Rayus Kuplicki<sup>a</sup>, Chibing Tan<sup>c</sup>, Bethany N. Hannafon<sup>e</sup>, Rajagopal Ramesh<sup>f</sup>, Jonathan Savitz<sup>a,d</sup>, Sahib Khalsa<sup>a,d</sup>, T. Kent Teague<sup>b,g,h</sup>, Victoria B. Risbrough<sup>i,j</sup>, Martin P. Paulus<sup>a,d</sup>

<sup>a</sup> Laureate Institute for Brain Research, Tulsa, OK, USA

<sup>b</sup> Departments of Surgery and Psychiatry, School of Community Medicine, The University of Oklahoma, Tulsa, OK, USA

<sup>c</sup> Integrative Immunology Center, School of Community Medicine, The University of Oklahoma, Tulsa, OK, USA

<sup>d</sup> Department of Community Medicine, The University of Tulsa, Tulsa, OK, USA

<sup>e</sup> Department of Obstetrics & Gynecology, The University of Oklahoma Health Sciences Center, Oklahoma City, OK, USA

<sup>f</sup> Department of Pathology, The University of Oklahoma Health Sciences Center, Oklahoma City, OK, USA

<sup>g</sup> Department of Biochemistry and Microbiology, The Oklahoma State University Center for Health Sciences, Tulsa, OK, USA

<sup>h</sup> Department of Pharmaceutical Sciences, The University of Oklahoma College of Pharmacy, Oklahoma City, OK, USA

<sup>i</sup> Center of Excellence for Stress and Mental Health, La Jolla, CA, USA

<sup>j</sup> Department of Psychiatry, University of California, San Diego, La Jolla, CA, USA

### ARTICLE INFO

#### Keywords:

Astrocyte-enriched extracellular vesicles  
miR-23b  
Ibuprofen  
Inflammation  
Reward processing  
Monetary incentive delay task  
fMRI  
TNF  
IL-17A

### ABSTRACT

Ibuprofen, a non-steroidal, anti-inflammatory drug, modulates inflammation but may also have neuroprotective effects on brain health that are poorly understood. Astrocyte-enriched extracellular vesicles (AEEVs) facilitate cell-to-cell communication and – among other functions - regulate inflammation and metabolism via micro-ribonucleic acids (miRNAs). Dysfunctions in reward-related processing and inflammation have been proposed to be critical pathophysiological pathways in individuals with mood disorders. This investigation examined whether changes in AEEV cargo induced by an anti-inflammatory agent results in inflammatory modulation that is associated with reward-related processing. Data from a double-blind, randomized, repeated-measures study in healthy volunteers were used to examine the effects of AEEV miRNAs on brain activation during reward-related processing. In three separate visits, healthy participants (N = 20) received a single dose of either placebo, 200 mg, or 600 mg of ibuprofen, completed the monetary incentive delay task during functional magnetic resonance imaging, and provided a blood sample for cytokine and AEEV collection. AEEV miRNA content profiling showed that ibuprofen dose-dependently increased AEEV miR-23b-3p expression with greater increase following the 600 mg administration than placebo. Those individuals who received 600 mg and showed the highest miR-23b-3p expression also showed the (a) lowest serum tumor necrosis factor (TNF) and interleukin-17A (IL-17A) concentrations; and had the (b) highest striatal brain activation during reward anticipation. These results support the hypothesis that ibuprofen alters the composition of miRNAs in AEEVs. This opens the possibility that AEEV cargo could be used to modulate brain processes that are important for mental health.

### 1. Introduction

Ibuprofen is a non-steroidal, anti-inflammatory drug (NSAID) with

anti-pyretic and anti-analgesic properties (Adams et al., 1969; Bushra and Aslam, 2010). The inhibition of cyclooxygenase (COX) activity explains ibuprofen's repressive effects on prostaglandin (PG) and cytokine

\* Corresponding author. Laureate Institute for Brain Research, 6655 South Yale Ave, Tulsa, OK, 74136, USA.

E-mail address: [kburrows@laureateinstitute.org](mailto:kburrows@laureateinstitute.org) (K. Burrows).

<sup>1</sup> Kaiping Burrows and Leandra K. Figueroa-Hall should be considered joint first author.

synthesis, ultimately leading to decreased fever, inflammation, and pain (Gunaydin and Bilge, 2018). Along with ibuprofen's ability to induce peripheral effects, it also shows the potential to be neuroprotective, attenuate proinflammatory mediators, and reduce glial cell populations including prevention of astrogliosis (Márquez Loza et al., 2017; Wixey et al., 2019). Importantly, COX-1 is expressed in glial white and gray matter and in regions such as the hippocampus and cortex, raising the possibility that ibuprofen could modulate cognitive processing (Gunaydin and Bilge, 2018; Shang et al., 2014; Sofroniew and Vinters, 2010; Zidar et al., 2009).

Astrocytes are emerging as one of the regulators of the central nervous system's (CNS) inflammatory responses, and therefore, may play a critical role in homeostasis and neurodegeneration (Sofroniew, 2015). Ibuprofen's direct effects on astrocytes were demonstrated in reduction of the astrocytic activation marker, glial fibrillary acidic protein (GFAP), in pre-clinical models (Lim et al., 2000; Peng et al., 2019; Rogers et al., 2017). Moreover, astrocytes respond to both pathogenic patterns and cellular content, enabling coordinated innate immune peripheral and central inflammatory responses, and thus, regulation by micro ribonucleic acids (miRNAs) is warranted (Carpentier et al., 2005; Figueroa-Hall et al., 2020; Nejad et al., 2018). In the healthy brain, astrocyte-mediated inflammatory signaling is involved in neuroplasticity; conversely, astrocyte-mediated pathological signaling leads to disruption of neural networks and neuroinflammation, including upregulation of inflammatory markers including cytokines and chemokines, which can lead to deficits in brain reward processing (Croitoru-Lamoury et al., 2003; Haber and Behrens, 2014; Jensen et al., 2013; Stellwagen and Malenka, 2006).

Reward-related processing modulates fundamental cognitive functions such as attention, memory, decision-making, and learning and can be measured by the monetary incentive delay (MID) task, which elicits robust striatal activation during anticipation of rewards (Hélie et al., 2017; Knutson et al., 2000, 2001; Wilson et al., 2018). Deficits in reward-related processing occur in a variety of mental disorders, such as major depressive disorder (MDD), and can lead to impaired valuation of reinforcers that prevent an individual from engaging in adaptive goal-directed action (Der-Avakian and Markou, 2012). Moreover, reward-related processing dysfunction is linked to poor treatment outcomes in clinical populations, such that individuals with MDD display deficits in brain reward processing in the form of decreased activity of ventral striatum (VS) (Epstein et al., 2006; Husain and Roiser, 2018; Pizzagalli et al., 2009; Takamura et al., 2017; Vinckier et al., 2017). In addition, astrocytes regulate reward processing in the brain reward system such as nucleus accumbens by mediating the dopamine- and amphetamine-induced synaptic regulation (Becker-Krail et al., 2022; Corkrum et al., 2020). Deficits in brain reward processing have been linked to inflammation in both pre-clinical and experimental human studies. For instance, elevated peripheral inflammation was associated with attenuated reward anticipation in MDD (Burrows et al., 2021; Han and Ham, 2021; Yin et al., 2019). Our previous study showed ibuprofen's ability to change the slope of association between brain reward processing and neuronally-enriched extracellular vesicle (EV) miR-27b (Burrows et al., 2022).

Ibuprofen's ability to rapidly cross the blood brain barrier (Parepally et al., 2006) and astrocytes' ability to regulate neuronal functions, led us to investigate AEEV miRNAs and their ability to modulate peripheral inflammation and brain reward processing using the MID gain vs. non-gain and loss vs. non-loss contrasts in the reward regions post ibuprofen treatment. miRNAs are a class of small non-coding RNAs that are key post-transcriptional regulators of gene expression. Astrocyte-identifying miRNAs, including miR-23, miR-26, and miR-29 have been reported in the brain in both gray and white matter (Luarte et al., 2017; Ouyang et al., 2014; Smirnova et al., 2005). miRNA regulation of astrocytes occurs partly through secreted extracellular vesicles (EVs), whose cargo can modulate astrocytic functions in health and disease (Varciana et al., 2019). EVs originating from astrocytic

multivesicular bodies, expressing glutamate aspartate transporter (GLAST), and ranging in size from 30 to 150 nanometers (nm) represent astrocyte-enriched (AE)EVs. AEEVs may play a role in maintaining neuronal functions, including maintenance of reward processing with the transfer of potentially protective and functional transmitter cargo (Gayen et al., 2020; Kastanenko et al., 2020; Lafourcade et al., 2016).

In this exploratory, follow-up from our previously published work (Burrows et al., 2022), we leveraged samples from a double-blind, randomized, within-subjects study that administered ibuprofen (placebo, 200 mg, and 600 mg; see Burrows et al., 2022) to healthy individuals to examine our exploratory hypotheses that ibuprofen modulates AEEV miRNAs and peripheral inflammatory cytokine profiles that can in turn, improve anticipation of rewards.

## 2. Materials and methods

### 2.1. Study design

The study design was previously published by Burrows and colleagues (Burrows et al., 2022). Briefly, twenty healthy subjects (10 females; mean age = 32 years, SD = 7, range = 27 to 51; mean body mass index [ $\text{kg}/\text{m}^2$ ] = 27, SD = 6, range = 20.4 to 44.7) completed a double-blind, randomized, repeated-measures study (Identifier on clinicaltrials.gov: NCT02507219, Study of Ibuprofen Effects on Brain Function). Sample characteristics of healthy subjects can be found in Burrows et al. Three previous manuscripts have been published on this study (Burrows et al., 2022; Cosgrove et al., 2021; Le et al., 2018). The study carried out at the Laureate Institute for Brain Research in Tulsa, Oklahoma, was approved by the Western Institutional Review Board and carried out in accordance with the principles in the Declaration of Helsinki; all participants provided written informed consent and received compensation for their participation. The CONSORT flow diagram can be found in the supplement, which describes eligibility, randomization, and analysis with reasons for subject exclusion (Supplemental Fig. S1). No adverse effects resulted in this study.

Ibuprofen and identical-looking placebo tablets were provided by a local pharmacy in Tulsa, OK. For random allocation, a statistician not involved in data collection provided a random number generator. All study personnel remained blinded until data collection was completed. Eligible subjects were tested three times. During each test session, subjects fasted overnight, arrived in the morning, and received one oral dose of placebo, 200 mg, or 600 mg of ibuprofen (dose order was counterbalanced across subjects). Subjects underwent a functional magnetic resonance imaging (fMRI) scan approximately 1 hour (h) after dosing and venous blood was collected 5 h after drug administration. Venous blood was collected in BD Vacutainer Serum Blood Collection tubes and centrifuged at  $1300\times g$  for 10 (min) at room temperature; serum was then removed, aliquoted, and stored at  $-80^\circ\text{C}$  until analysis.

### 2.2. Astrocyte-enriched extracellular vesicles (AEEVs)

#### 2.2.1. AEEV isolation

We have submitted all relevant data of our experiments to the EV-TRACK knowledgebase (EV-TRACK ID: 220014) (Van Deun et al., 2017). Total extracellular vesicles (TEs) were isolated using ExoQuick Exosome Precipitation Solution (EPS; System Biosciences, CA, United States; Catalog #EXOQ5A-1) as previously described (Burrows et al., 2022). Briefly, 250  $\mu\text{L}$  of frozen serum samples were incubated with 63  $\mu\text{L}$  of ExoQuick EPS on ice for 30 min; resultant suspensions were centrifuged at  $1500\times g$  for 30 min at  $4^\circ\text{C}$ . TEV pellets were re-suspended in 300  $\mu\text{L}$  of 1X phosphate buffered saline (PBS) with Halt protease and ethylenediaminetetraacetic acid (EDTA)-free phosphatase inhibitor cocktail. Subsequently, TEs were enriched by a magnetic streptavidin bead immunocapture kit against the astrocyte marker, astrocyte cell surface antigen-1 (ACSA-1) biotinylated antibody (Miltenyi Biotec, Inc., United States; Catalog # 130-118-984). Next, 80  $\mu\text{L}$  of 9.1  $\mu\text{m}$  covalently

cross-linked streptavidin magnetic beads (System Biosciences, CA, United States; Catalog #CSFLOWBASICA-1) and 20  $\mu\text{L}$  of 100 ng/ $\mu\text{L}$  of mouse anti-human ACSA-1 biotinylated antibody were incubated on ice for 2 h with gentle flicking every 30 min. After washing three times in 1X Bead Wash Buffer (BWB) (Systems Biosciences, CA, United States; Catalog #CSFLOWBASICA-1) using a magnetic stand, the bead/antibody complex was resuspended in 400  $\mu\text{L}$  of BWB. 200  $\mu\text{L}$  of TE suspensions were added to the bead/antibody complex and incubated overnight at 4  $^{\circ}\text{C}$  with rotation. See Fig. 1A for the schematic depiction of AEEV enrichment.

### 2.2.2. Flow cytometry

The bead/antibody/EV complex was (a) coupled to a fluorescein isothiocyanate (FITC) fluorescent tag that binds to extracellular vesicles (Exo-FITC, Systems Biosciences; Cat #CSFLOWBASICA-1) and a phycoerythrin (PE) fluorescent tag that specifically binds to the astrocyte surface marker, GLAST-PE (Miltenyi Biotec Inc; Cat #130-118-483); and (b) subsequently analyzed by flow cytometry to confirm AEEV capture. The bead/antibody/EV complex was washed three times with 1X BWB and then incubated with 10  $\mu\text{L}$  of Exo-FITC and 2  $\mu\text{L}$  of GLAST-PE in 240  $\mu\text{L}$  of Exosome Stain Buffer for 2 h on ice with gentle flicking every 30 min. The stained complex was washed three times in 1X BWB and resuspended in 500  $\mu\text{L}$  1X BWB prior to flow cytometry analysis. The flow cytometric data were acquired using a BD LSR II Special Order Flow Cytometer (BD Biosciences, San Jose, CA). Instrument performance was validated using BDTM Cytometer Setup and Tracking (CS&T) beads (BD Biosciences, San Jose, CA). All data were analyzed using FACS DIVA 8.0 software (BD Biosciences). Debris and small particles were excluded by gating out events with low forward scatter. Fig. 1B shows an example of successful EV capture, and Fig. 1C shows an example of AEEV enrichment.

### 2.2.3. Nanoparticle size analysis

The concentration and size of AEEVs were measured using microfluidic resistive pulse sensing (MRPS) with the Spectradyne nCS1<sup>TM</sup>

instrument. The samples were first diluted 1:2 in a 20 nm filtered solution of 1X PBS with 1% polysorbate 20 (Tween-20). Small volume of the final solution (5  $\mu\text{L}$ ) was analyzed using C-400 cartridges (range 65–400 nm particle size) and the data processed using Spectradyne software. Fig. 1D showed that the majority of captured AEEVs were in the EV size range; the average concentration of AEEVs was approximately  $2 \times 10^9$  particles per mL.

2.2.4 Western Blot. Enrichment of TE and AEEV was confirmed by western blot (Fig. 1E) as previously described by Burrows K. et al. (Burrows et al., 2022). Samples for western blot consisted of (from left to right): AEEV #1, total EV, EV-depleted serum (serum after Exoquick), AEEV #2, no EV (PBS/elution buffer), and AEEV #3. Briefly, 15  $\mu\text{g}$  of protein was denatured in reducing sample buffer and separated by 4–20% polyacrylamide gel. Following electrophoresis, gel was transferred onto polyvinylidene difluoride (PVDF) membrane using the Trans-Blot<sup>®</sup> Turbo Transfer System (Bio-Rad, USA, Catalog # 1704156). After semi-dry transfer, PVDF membranes were blocked with 5% non-fat dry milk in Tris-buffered saline containing 0.1% Tween-20 (TBS-T) for 1 h and then incubated with primary anti-GLAST antibody (1:1000, Clone 8C11.1, EMD Millipore, Catalog # MABN794) in TBS-T with 1% BSA overnight at 4  $^{\circ}\text{C}$ . After three washes, PVDF membranes were incubated with horseradish-peroxidase-conjugated anti-mouse antibody (1:2000, Cell Signaling, catalog 7076S) in TBS-T with 1% BSA for 1 h at room temperature. PVDF membranes were then visualized by Clarity Max Western ECL Substrate (Bio-Rad, USA, Catalog # 1705062) and imaged using ImageQuant LAS 4000 (GE Healthcare BioScience, Sweden). The image displayed in Fig. 1E was from the same gel without cutting prior to antibody hybridizations, see Supplemental Fig. S2 for the image of full-length gel.

### 2.2.4. AEEV miRNA purification

Purification of miRNA from AEEV was conducted using a Qiagen miRNeasy Micro Kit (QIAGEN, United States; Catalog #217084) according to the manufacturer's protocol. Small RNA concentration was measured using an Agilent Small RNA Kit (Agilent, United States;

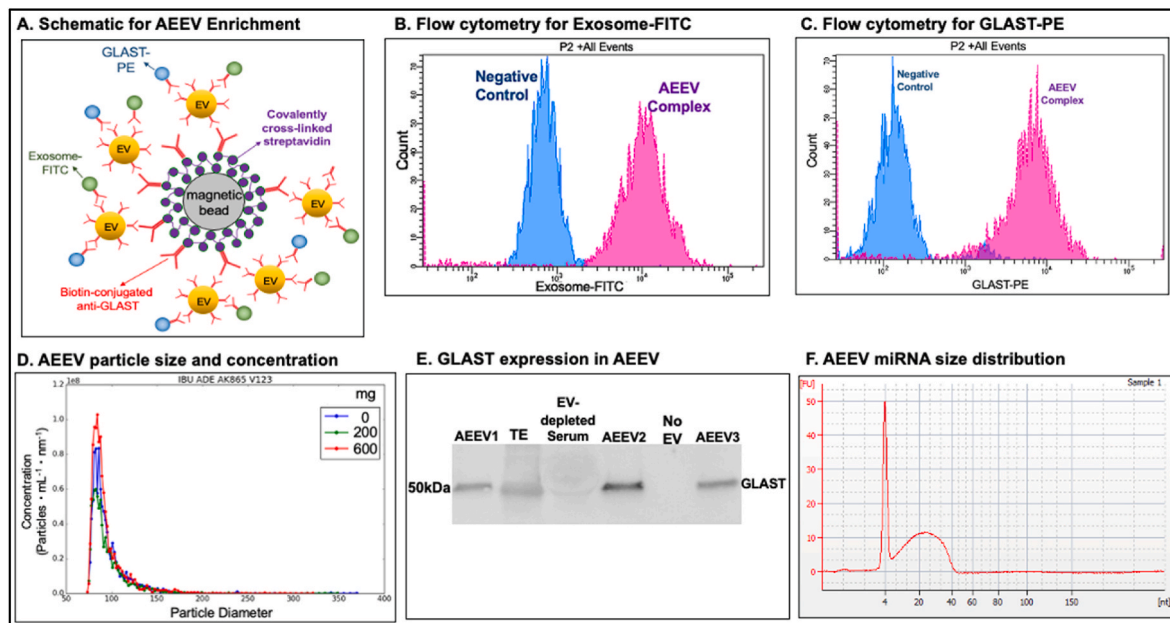


**Fig. 1.** Astrocyte-enriched extracellular vesicle (AEEV) enrichment. Note. A. Schematic depiction of AEEV enrichment. TEs isolated from serum were enriched by 9.1  $\mu\text{m}$  magnetic streptavidin beads against the astrocyte cell surface antigen-1 (ACSA-1, GLAST) biotinylated antibody, and then coupled to a fluorescein isothiocyanate (FITC) fluorescent tag that only binds to EVs (Exosome-FITC) and a phycoerythrin (PE) fluorescent tag that binds to astrocyte surface (GLAST-PE). B. Flow cytometry (FC) results of AEEVs and negative control on Exosome-FITC. C. FC results of AEEVs and negative control on GLAST-PE. D. Particle size and concentration analysis of AEEVs using the Spectradyne nCS1 (microfluidic resistive pulse sensing-MRPS). E. Western blot analysis of AEEVs, TE, EV-depleted serum, and negative controls (No EV) with anti-GLAST antibody marker, image cropped was from the same gel. F. AEEV miRNA concentration measured by an Agilent Small RNA Kit on a Bioanalyzer 2100 instrument.

Catalog #5067-1548) on a Bioanalyzer 2100 instrument (Agilent, United States) an example of AEEV miRNA concentration was shown in Fig. 1F, the miRNA concentration is 2601 pg/ $\mu$ L with a miRNA to small RNA ratio of 96%, which confirms isolation of enriched small RNAs from the AEEV samples. miRNA samples were stored at  $-80^{\circ}\text{C}$  until sequencing.

### 2.2.5. AEEV miRNA sequencing and data processing

miRNA samples were sent to the Oklahoma Medical Research Foundation (OMRF) Clinical Genomics Center for sequencing. The miRNA libraries were generated with a Qiagen QIAseq miRNA library preparation kit and sequencing performed on an Illumina NextSeq HO SR75. Raw sequence FASTQ files received from OMRF were imported to Partek Flow software for data analysis. Briefly, adapters from 3' end were trimmed from the raw read after a quality check, and then aligned to the human genome hg38 using Bowtie alignment. Next, the aligned reads were quantified against the human miRbase mature microRNAs version 22. Reads from miRNA genes were normalized, scaled to counts per million, and added 1 for statistical analysis.

### 2.3. Immunoassays

Serum inflammation-related markers were measured with the V-Plex Neuroinflammation Panel 1 Human Kit (#K15210D-1; Meso Scale Diagnostics, Maryland, USA). Samples from individual subjects were tested on the same plate in duplicate. See Supplemental Table S1 for full list of markers and the mean intra-assay coefficients of variation (CV). Interleukin (IL)-13, IL-1 alpha, IL-1 beta, IL-2, IL-4, and tumor necrosis factor (TNF)-beta were excluded from analysis due to detection rate less than 90%. The following analytes with an intra-assay CV < 10% were used for analysis: C-reactive protein (CRP), eotaxin, eotaxin-3, basic fibroblast growth factor (bFGF), vascular endothelial growth factor receptor 1 (VEGFR-1), soluble intercellular adhesion molecule 1 (sICAM-1), interferon (IFN) gamma (IFN- $\gamma$ ), IL-10, IL-12, IL-15, IL-16, IL-17A, IL-5, IL-6, IL-7, IL-8, IFN $\gamma$ -induced protein 10 (IP-10), monocyte chemoattractant protein-1 (MCP-1), monocyte chemoattractant protein-4 (MCP-4), C-C motif chemokine 22 (MDC), macrophage inflammatory protein-1 alpha (MIP-1 $\alpha$ ), macrophage inflammatory protein-1 beta (MIP-1 $\beta$ ), placental growth factor (PLGF), serum amyloid A (SAA), chemokine (C-C motif) ligand 17 (TARC), angiopoietin-1 receptor (Tie-2), TNF- $\alpha$ , soluble vascular cell adhesion molecule 1 (sVCAM-1), vascular endothelial growth factor A (VEGF-A), vascular endothelial growth factor C (VEGF-C), and vascular endothelial growth factor D (VEGF-D).

### 2.4. Neuroimaging

#### 2.4.1. fMRI MID task

At each session, subjects completed two runs of the MID task (Knutson et al., 2001). Each run included 45 trials and lasted 562 s. On each trial, a cue indicated a potential win (circle) or loss (square) along with a magnitude of 0, 1, or 5 US dollars. Following a short delay period, subjects were asked to respond to a target (white triangle) stimulus within a short time to win or avoid losing the amount indicated by the cue. Task difficulty was calibrated using each subject's reaction time measured during a practice session and further adjusted during scanning so that subjects would succeed on approximately 67% of the trials.

#### 2.4.2. fMRI data acquisition and preprocessing

The functional and structural MRI images were acquired on two identical GE MR750 3T scanners. A brain-dedicated receive-only 8-element coil array (General Electric), optimized for parallel imaging was used for MRI signal reception. A single-shot gradient-recalled echoplanar imaging (EPI) sequence with Sensitivity Encoding (SENSE) was used for blood oxygenation level dependent (BOLD) fMRI imaging. The EPI imaging parameters were TR/TE = 2000/27 ms, FOV/slice = 240/2.9 mm, 128  $\times$  128 matrix, and 39 axial slices. High resolution structural

images were also acquired with T1-weighted magnetization prepared rapid acquisition with gradient-echo (MPRAGE) sequence with SENSE. The anatomical scan had the following parameters: TR/TE = 5/2.012 ms, FOV/slice = 240  $\times$  192/0.9mm, 186 axial slices and a 256 $\times$ 256 reconstruction matrix producing 0.938  $\times$  0.938  $\times$  0.9 mm voxels. Functional image data preprocessing was performed using the AFNI software package (Cox, 1996). The EPI volumes underwent slice timing correction, alignment to anatomical volumes, rigid body motion correction, smoothing with a 4 mm full-width at half-maximum Gaussian kernel and normalization to Montreal Neurological Institute space with a final voxel size of 2  $\times$  2  $\times$  2 mm. The first three volumes were discarded to allow the fMRI signal to reach longitudinal equilibrium. Signal intensity was normalized to reflect percent signal change from each voxel's mean intensity across the time-course. Four-second block regressors were convolved with a canonical hemodynamic response function and used to model the BOLD response to each of the six anticipatory task conditions: 5, -1, -0, +0, +1, +5. Additionally, the model included regressors of non-interest to account for each run's mean, linear, quadratic, and cubic signal trends, as well as the 6 normalized motion parameters (3 translations, 3 rotations) computed during the image registration. The gain vs. non-gain contrast consisted of the average signal change across small and large wins (+1 and +5) minus the no win (+0) condition. The loss vs. non-loss contrast consisted of the average signal change across small and large losses (-1 and -5) minus the no loss (-0) condition.

### 2.5. Gene Set Enrichment Analysis (GSEA) biological pathway analysis

2.5.1 To understand the relevance and functional aspects of AEEV miR-23b-3p in relation to this study, the biological pathway analysis was performed with miRWalk (Ding et al., 2017). For this, target mining of the full mature miRNA, hsa-miR-23b-3p, was searched with miRBaseID. Next, designating the 3' UTR, two filters were set for the GSEA analysis: TargetScan and miRDB.

### 2.6. Statistical analysis

#### 2.6.1. AEEV miRNAs

Normalized miRNA gene miR-23b-3p was log-transformed and used as the dependent variable in a repeated measures analysis of variance (ANOVA) with dose (placebo, ibuprofen 200 mg, ibuprofen 600 mg) as the within-subjects variable; paired t-tests were employed to test mean differences between doses. Identical ANOVAs were also estimated for 19 other miRNAs with enough counts for statistical analysis; specifically, miRNAs with more than two missing values (10% of sample size) were excluded from analysis.

#### 2.6.2. Exploratory correlations between miR-23b-3p and inflammatory markers

Shapiro-Wilks tests were used to test normality of distributions for each useable inflammatory marker; those that were found to be non-Gaussian were log-transformed.

#### 2.6.3. MID condition analyses

AFNI's group analysis program 3dtest++ was used to evaluate the relationship between miR-23b-3p and percent fMRI BOLD signal change on the MID gain vs. non-gain and loss vs. non-loss contrasts within ibuprofen doses on miR-23b-3p. The family wise error rate was set to  $\alpha < 0.05$  using AFNI's 3dClustsim -acf function to estimate probability of false positives. Multiple comparisons were performed by applying this cluster-wise correction to the following Region of Interest (ROI) related to reward processing: left and right insula, thalamus, caudate, putamen, and nucleus accumbens that were selected a priori, as well as the whole brain outside of those ROIs. In addition, repeated measures ANOVAs tested dose differences on reaction time and hit rate for MID task performance.

### 3. Results

#### 3.1. Astrocyte-enriched extracellular vesicles (AEEV) miRNA

There was a main effect of ibuprofen dose on AEEV miR-23b-3p ( $F_{1,18} = 7.47, p = 0.004$ , Fig. 2). Pairwise comparisons indicated that ibuprofen 600 mg exhibited higher miR-23b-3p expression ( $p < 0.001$ , Cohen's  $d$  ( $d$ ) = 0.84) than placebo.

Supplemental Table S2 lists additional miRNAs detected in AEEVs. The effect of ibuprofen was not limited to the above miRNA but also included 19 other miRNAs. Specifically, ibuprofen 600 mg resulted in higher miR-27b-3p expression ( $p = 0.02$ ) than placebo. However, none of the miRNAs survived correction for multiple comparisons.

#### 3.2. Relationship between AEEV miR-23b-3p and inflammation-related biomarkers

Because there was a significant difference between placebo and ibuprofen 600 mg on miR-23b-3p, Pearson's correlation was used to explore potential relationships between miR-23b-3p and useable inflammatory markers within placebo and ibuprofen 600 mg. At the 600 mg ibuprofen dose, higher miR-23b-3p expression was associated with lower TNF ( $r = -0.516, p = 0.020$ ) and IL-17A ( $r = -0.478, p = 0.033$ ) concentrations, but not in placebo condition (Fig. 3). In addition, higher miR-23b-3p expression was associated with lower IL-10 ( $r = -0.540, p = 0.014$ ) concentrations at 600 mg ibuprofen dose.

See Supplemental Table S3 for correlations between miR-23b-3p and inflammatory markers. No significant relationships were found between miR-23b-3p and any of the inflammatory markers in the placebo condition.

#### 3.3. Relationship between AEEV miR-23b-3p and reward processing

Fig. 4A shows that there was a significant positive correlation between miR-23b-3p and the MID gain vs. non-gain contrast within right dorsal caudate ( $r = 0.656, p = 0.002$ ) and anterior cingulate cortex ( $r = 0.799, p < 0.001$ ) at the 600 mg ibuprofen dose, while no such relationship was observed for the placebo dose. In addition, partial correlations showed a similar significant positive relationship between miR-

23b-3p and the gain vs. non-gain contrast within right dorsal caudate ( $r = 0.507, p = 0.027$ ) and anterior cingulate cortex ( $r = 0.727, p < 0.001$ ) at 600 mg ibuprofen dose after controlling for TNF concentrations. Similarly, partial correlations at the 600 mg ibuprofen dose showed that the positive relationship between miR-23b-3p and the gain vs. non-gain contrast within the right dorsal caudate ( $r = 0.514, p = 0.024$ ) and anterior cingulate cortex ( $r = 0.731, p < 0.001$ ) remained after controlling for IL-17 concentrations.

A significant negative correlation was observed between miR-23b-3p and the MID loss vs. non-loss contrast within right thalamus ( $r = -0.641, p = 0.002$ ) at the 600 mg ibuprofen dose, while no such relationship was observed for the placebo dose (Fig. 4B). Partial correlations showed a similar significant negative relationship between miR-23b-3p and the loss vs. non-loss contrast within right thalamus at 600 mg ibuprofen dose after controlling for TNF ( $r = -0.499, p = 0.030$ ) or for IL-17 ( $r = -0.590, p = 0.008$ ) concentrations.

Supplemental Table S4 shows the peak coordinates, t-values and volumes for regions exhibiting significant correlations between AEEV miR-23b and % fMRI signal change for the MID gain vs. no gain contrast within ibuprofen dose 600 mg in the voxel-wise whole brain analysis. In addition, subjects' task performance on reaction times and correct hits did not differ between doses (Supplemental Table S5).

#### 3.4. AEEV-miR23b-mediated biological pathway

Gene Set Enrichment Analysis (GSEA) Biological Pathway Analysis for AEEV miR-23b-3p using miRWalk identified 153 genes (Fig. 5) and 36 biological pathways, of which 25 were statistically significant after Bonferroni correction (Supplemental Table S6).

### 4. Discussion

This study examined the hypothesis whether ibuprofen modulated AEEV miRNA content and peripheral inflammatory markers, which could alter brain reward-related processing. There were three main findings. First, acute administration of 600 mg ibuprofen relative to placebo resulted in a higher miR-23b-3p expression. Second, those individuals with higher AEEV miR-23b-3p after acute administration of 600 mg of Ibuprofen but not after placebo or 200 mg, were associated with lower TNF and IL-17 serum protein concentrations. This association is consistent with the role of miR-23b in regulating inflammatory cytokines (Luo et al., 2021; Zhang et al., 2019; Zhu et al., 2012). Third, those individuals with higher AEEV miR-23b-3p after acute administration of 600 mg of ibuprofen but not after placebo or 200 mg, showed greater brain activation in the striatum and anterior cingulate during the MID gain vs. non-gain condition and lowest brain activations in thalamus during the MID loss vs. no-loss condition. This finding is consistent with the proposed negative influence of immune signaling on reward-related processing and the potential of Ibuprofen to ameliorate this dysfunction. Taken together, these findings provide evidence for the ibuprofen-mediated effects of AEEV miR-23b and inflammatory proteins – possibly having independent cognitive-mediated regulatory effects. Future studies will evaluate whether AEEV miR-23b mediates intercellular astrocyte communication with the use of *in vitro* studies.

600 mg of ibuprofen increased the expression of miR-23b, which is similar to results found with ibuprofen treatment of human synovial fibroblasts or patients with osteoarthritis leading to increased expression of miRNAs and reduction of mRNA and protein levels of IL-6, TNF, and IL-1 $\beta$  (Gallelli et al., 2013; Law et al., 2021). Similar to our findings, Sayin N et al., found that treatment of isolated human mononuclear cells with ibuprofen inhibited TNF and IL-17 (Sayin, 2013). IL-17, a molecule found to be increased in the blood of depressed individuals (Davami et al., 2016), upregulates activation of inflammatory transcription factors, NF- $\kappa$ B and mitogen activated protein kinase (MAPK), and production of PGE2, IL-6, IL-8, ICAM-1, and matrix metalloproteinase 9 (MMP-9), amongst others (Li et al., 2019).

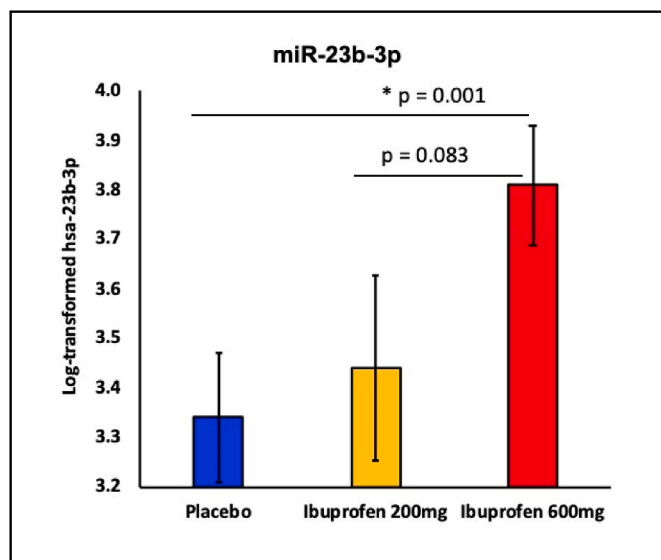
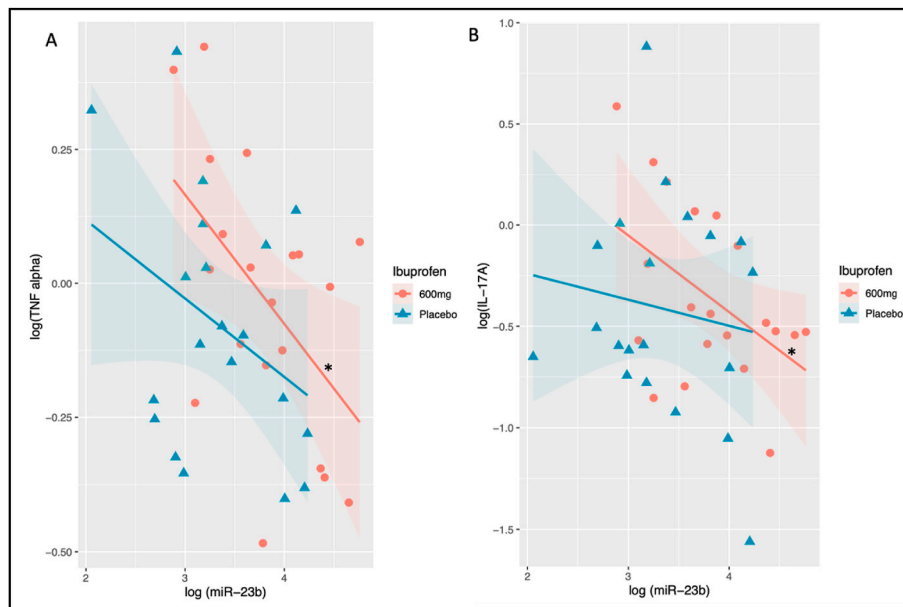
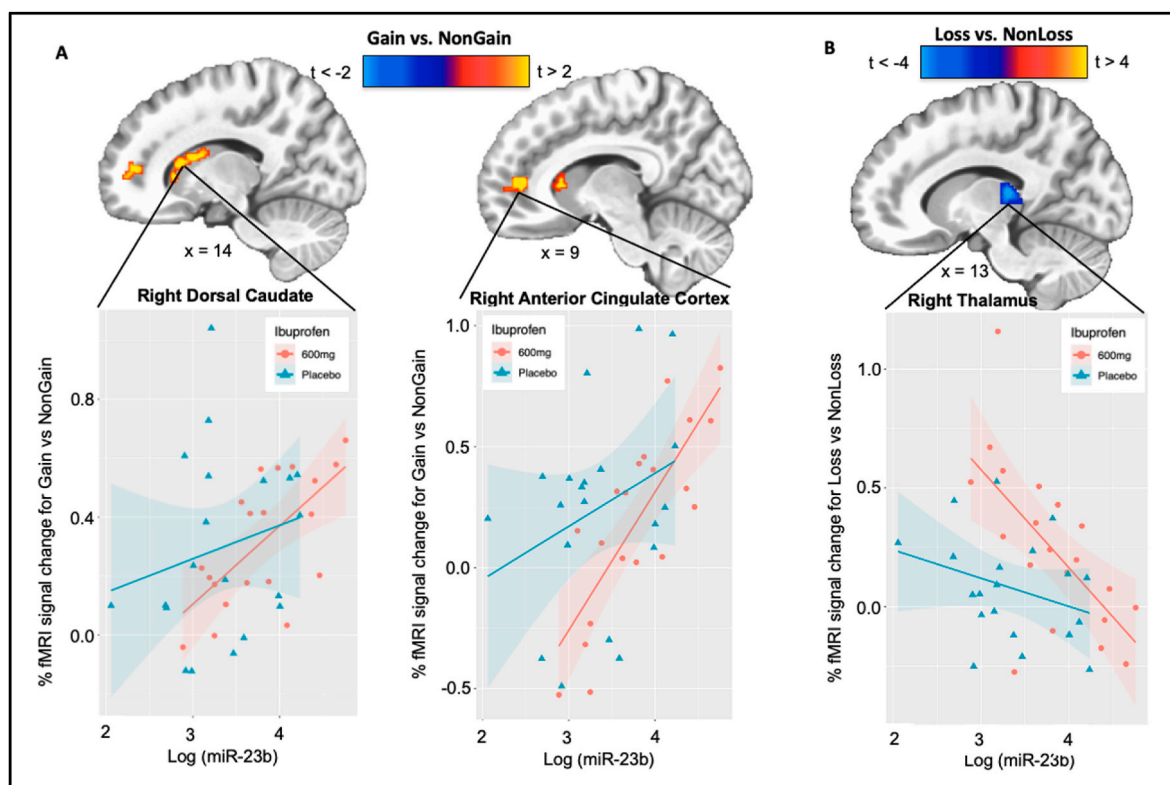


Fig. 2. Ibuprofen-mediated effect on AEEV miR-23b. Log-transformed data shows ibuprofen-mediated (200 and 600 mg) effects on astrocyte-enriched extracellular vesicles miRNA expression for miR-23b-3p; ( $N = 20$ ). Ibuprofen (600 mg) was significantly different from placebo ( $p = 0.001$ ). \* Denotes significant differences between conditions using paired  $t$ -test.



**Fig. 3. Correlations between AEEV miR-23b and inflammatory biomarkers.** A. At ibuprofen (600 mg), higher mir-23b expression was associated with lower TNF $\alpha$  ( $r = -0.539, p = 0.014$ ) but not placebo. B. Ibuprofen (600 mg) was negatively correlated with IL-17A ( $r = -0.478, p = 0.033$ ) but not placebo; (N = 20).



**Fig. 4. A.** Correlations between AEEV miR-23b and % fMRI signal change for the MID gain vs. no gain contrast at the 600 mg dose and placebo. **B.** Correlations between AEEV miR-23b and % fMRI signal change for the MID loss vs. no loss contrast at the 600 mg dose and placebo.

Human miRNAs are predominantly negative regulators of gene expression and are known to target molecular functions including protein, nucleic acid and DNA binding, and receptor, kinase, and transcription regulation activity (Lewis et al., 2003). As in our case and that of others, negative correlations of increased miRNA expression and decreased inflammatory markers could be attributed to miRNA-mediated negative regulation of several pathways including

NF- $\kappa$ B, MAPK, and signal transducer and activator of transcription 3 (STAT3) (Gallelli et al., 2013; Sun et al., 2017). For example, IL-17 signaling, which shares homology with TLR signaling, contains downstream proteins, such as TNF receptor associated factor 6 (TRAF6) and transforming growth factor beta (TGF- $\beta$ )-activated kinase 1 (TAK1) that are potential targets for miRNA regulation. Relevant to our findings, miR-23b has been shown to target TAK1 binding protein 2 (TAB2),



Medical Sciences Center Grant Award (P20GM121312 to MPP).

### Author contributions

K.B. contributed to research design, data collection, data analysis, and manuscript writing, preparation, and review; L.K.F. contributed to data analysis, manuscript writing, preparation, and review; A.M.A. contributed to EV western blot analysis, manuscript writing and preparation; J.L.S. contributed to manuscript writing and preparation; R.K. contributed to imaging data collection and analysis, manuscript writing and preparation; C.T. contributed to EV flow cytometry data collection and analysis; B.N.H. contributed to EV isolation protocols, western blot troubleshooting, and reviewing of the manuscript;

R.R. contributed to EV nanoparticle analysis, review and editing of the manuscript; J.B.S. contributed to critical manuscript review; S.K. contributed to critical manuscript review; T.K.T. contributed to study design, EV western blot and flow cytometry analysis, critical manuscript writing and review; V.B.R. contributed to EV study design, supervision of EV data collection and analysis; M.P.P. contributed to study design, supervision of data collection and analysis, manuscript writing and preparation, and critical review of the manuscript. All authors reviewed the manuscript.

### Declaration of competing interest

All authors have no competing financial interests as it relates to the work represented in this manuscript.

### Data availability

Data will be made available on request.

### Acknowledgements

The blood processing and EV isolation were conducted at the Integrative Immunology Center (IIC), School of Community Medicine, The University of Oklahoma, Tulsa, OK. The authors wish to thank the IIC staff Ashlee Rempel and Brenda Davis for their work and support involved in the data collection.

### Appendix A. Supplementary data

Supplementary data to this article can be found online at <https://doi.org/10.1016/j.bbih.2022.100582>.

### References

- Adams, S.S., McCullough, K.F., Nicholson, J.S., 1969. The pharmacological properties of ibuprofen, an anti-inflammatory, analgesic and antipyretic agent. *Arch. Int. Pharmacodyn. Ther.* 178, 115–129.
- Becker-Krahl, D.D., Ketchesin, K.D., Burns, J.N., Zong, W., Hildebrand, M.A., DePoy, L. M., Vадnie, C.A., Tseng, G.C., Logan, R.W., Huang, Y.H., McClung, C.A., 2022. Astrocyte molecular clock function in the nucleus accumbens is important for reward-related behavior. *Biol. Psychiatr.* 92, 68–80.
- Burrows, K., Figueroa-Hall, L.K., Kuplicki, R., Stewart, J.L., Alarbi, A.M., Ramesh, R., Savitz, J.B., Teague, T.K., Risbrough, V.B., Paulus, M.P., 2022. Neuronally-enriched exosomal microRNA-27b mediates acute effects of ibuprofen on reward-related brain activity in healthy adults: a randomized, placebo-controlled, double-blind trial. *Sci. Rep.* 12, 861.
- Burrows, K., Stewart, J.L., Kuplicki, R., Figueroa-Hall, L., Spechler, P.A., Zheng, H., Guinjoan, S.M., Savitz, J.B., Kent Teague, T., Paulus, M.P., 2021. Elevated peripheral inflammation is associated with attenuated striatal reward anticipation in major depressive disorder. *Brain Behav. Immun.* 93, 214–225.
- Bushra, R., Aslam, N., 2010. An overview of clinical pharmacology of Ibuprofen. *Oman Med. J.* 25, 155–1661.
- Carpentier, P.A., Begolka, W.S., Olson, J.K., Elhofy, A., Karpus, W.J., Miller, S.D., 2005. Differential activation of astrocytes by innate and adaptive immune stimuli. *Glia* 49, 360–374.
- Christopherson, K.S., Ullian, E.M., Stokes, C.C.A., Mullaney, C.E., Hell, J.W., Agah, A., Lawler, J., Mosher, D.F., Bornstein, P., Barres, B.A., 2005. Thrombospondins are astrocyte-secreted proteins that promote CNS synaptogenesis. *Cell* 120, 421–433.
- Corkrum, M., Covelo, A., Lines, J., Bellocchio, L., Pisansky, M., Loke, K., Quintana, R., Rothwell, P.E., Lujan, R., Marsicano, G., Martin, E.D., Thomas, M.J., Kofuji, P., Araque, A., 2020. Dopamine-evoked synaptic regulation in the nucleus accumbens requires astrocyte activity. *Neuron* 105, 1036–1047 e1035.
- Cosgrove, K.T., Kuplicki, R., Savitz, J., Burrows, K., Simmons, W.K., Khalsa, S.S., Teague, T.K., Aupperle, R.L., Paulus, M.P., 2021. Impact of ibuprofen and peroxisome proliferator-activated receptor gamma on emotion-related neural activation: a randomized, placebo-controlled trial. *Brain Behav. Immun.* 96, 135–142.
- Cox, R.W., 1996. AFNI: software for analysis and visualization of functional magnetic resonance neuroimages. *Comput. Biomed. Res.* 29, 162–173.
- Croitoru-Lamoury, J., Guillemin, G.J., Boussin, F.D., Mognetti, B., Gigout, L.I., Chéret, A., Vaslin, B., Le Grand, R., Brew, B.J., Dormont, D., 2003. Expression of chemokines and their receptors in human and simian astrocytes: evidence for a central role of TNF alpha and IFN gamma in CXCR4 and CCR5 modulation. *Glia* 41, 354–370.
- Davami, M.H., Baharlou, R., Ahmadi Vasmehjani, A., Ghanizadeh, A., Keshtkar, M., Dezhkam, I., Atashzar, M.R., 2016. Elevated IL-17 and TGF- $\beta$  serum levels: a positive correlation between T-helper 17 cell-related pro-inflammatory responses with major depressive disorder. *Basic Clin. Neurosci.* 7, 137–142.
- Der-Avakian, A., Markou, A., 2012. The neurobiology of anhedonia and other reward-related deficits. *Trends Neurosci.* 35, 68–77.
- Ding, L., Ni, J., Yang, F., Huang, L., Deng, H., Wu, Y., Ding, X., Tang, J., 2017. Promising therapeutic role of miR-27b in tumor. *Tumour Biol* 39, 1010428317691657.
- Duke-Cohan, J.S., Gu, J., McLaughlin, D.F., Xu, Y., Freeman, G.J., Schlossman, S.F., 1998. Attractin (DPPT-L), a member of the CUB family of cell adhesion and guidance proteins, is secreted by activated human T lymphocytes and modulates immune cell interactions. *Proc. Natl. Acad. Sci. U. S. A.* 95, 11336–11341.
- Epstein, J., Pan, H., Kocsis, J.H., Yang, Y., Butler, T., Chusid, J., Hochberg, H., Murrough, J., Strohmayr, E., Stern, E., Silbersweig, D.A., 2006. Lack of ventral striatal response to positive stimuli in depressed versus normal subjects. *Am. J. Psychiatr.* 163, 1784–1790.
- Figueroa-Hall, L.K., Paulus, M.P., Savitz, J., 2020. Toll-like receptor signaling in depression. *Psychoneuroendocrinology* 121, 104843.
- Gallelli, L., Galasso, O., Falcone, D., Southworth, S., Greco, M., Ventura, V., Romualdi, P., Corigliano, A., Terracciano, R., Savino, R., Gulletta, E., Gasparini, G., De Sarro, G., 2013. The effects of nonsteroidal anti-inflammatory drugs on clinical outcomes, synovial fluid cytokine concentration and signal transduction pathways in knee osteoarthritis. A randomized open label trial. *Osteoarthritis Cartilage* 21, 1400–1408.
- Gayen, M., Bhomia, M., Balakathiresan, N., Knollmann-Ritschel, B., 2020. Exosomal MicroRNAs released by activated astrocytes as potential neuroinflammatory biomarkers. *Int. J. Mol. Sci.* 21.
- Gunaydin, C., Bilge, S.S., 2018. Effects of nonsteroidal anti-inflammatory drugs at the molecular level. *Eurasian J Med* 50, 116–121.
- Haber, S.N., Behrens, T.E.J., 2014. The neural network underlying incentive-based learning: implications for interpreting circuit disruptions in psychiatric disorders. *Neuron* 83, 1019–1039.
- Halahakoon, D.C., Kieslich, K., O'Driscoll, C., Nair, A., Lewis, G., Roiser, J.P., 2020. Reward-processing behavior in depressed participants relative to healthy volunteers: a systematic review and meta-analysis. *JAMA Psychiatr.*
- Han, K.-M., Ham, B.-J., 2021. How inflammation affects the brain in depression: a review of functional and structural MRI studies. *J. Clin. Neurol.* 17, 503–515.
- Hélie, S., Shamloo, F., Novak, K., Foti, D., 2017. The roles of valuation and reward processing in cognitive function and psychiatric disorders. *Ann. N. Y. Acad. Sci.* 1395, 33–48.
- Husain, M., Roiser, J.P., 2018. Neuroscience of apathy and anhedonia: a transdiagnostic approach. *Nat. Rev. Neurosci.* 19, 470–484.
- Jensen, C.J., Massie, A., De Keyser, J., 2013. Immune players in the CNS: the astrocyte. *J. Neuroimmune Pharmacol.* 8, 824–839.
- Kastanienka, K.V., Moreno-Bote, R., De Pittà, M., Perea, G., Eraso-Pichot, A., Masgrau, R., Poskanzer, K.E., Galea, E., 2020. A roadmap to integrate astrocytes into Systems Neuroscience. *Glia* 68, 5–26.
- Kerkerian, L., Nieouillon, A., Dusticier, N., 1982. Brain glutamate uptake: regional distribution study from sensorimotor areas in the cat. *Neurochem. Int.* 4, 275–281.
- Khakh, B.S., Sofroniew, M.V., 2015. Diversity of astrocyte functions and phenotypes in neural circuits. *Nat. Neurosci.* 18, 942–952.
- Knutson, B., Fong, G.W., Adams, C.M., Varner, J.L., Hommer, D., 2001. Dissociation of reward anticipation and outcome with event-related fMRI. *Neuroreport* 12, 3683–3687.
- Knutson, B., Westdorp, A., Kaiser, E., Hommer, D., 2000. fMRI visualization of brain activity during a monetary incentive delay task. *Neuroimage* 12, 20–27.
- Lafourcade, C., Ramirez, J.P., Luarte, A., Fernández, A., Wyneken, U., 2016. miRNAs in astrocyte-derived exosomes as possible mediators of neuronal plasticity. *J. Exp. Neurosci.* 10, 1–9.
- Law, Y.Y., Lee, W.F., Hsu, C.J., Lin, Y.Y., Tsai, C.H., Huang, C.C., Wu, M.H., Tang, C.H., Liu, J.F., 2021. miR-let-7c-5p and miR-149-5p inhibit proinflammatory cytokine production in osteoarthritis and rheumatoid arthritis synovial fibroblasts. *Aging (Albany NY)* 13, 17227–17236.
- Le, T.T., Kuplicki, R., Yeh, H.-W., Aupperle, R.L., Khalsa, S.S., Simmons, W.K., Paulus, M. P., 2018. Effect of ibuprofen on BrainAGE: a randomized, placebo-controlled, dose-response exploratory study. *Biol. Psychiatr.: Cognitive Neuroscience and Neuroimaging* 3, 836–843.
- Lewis, B.P., Shih, I.H., Jones-Rhoades, M.W., Bartel, D.P., Burge, C.B., 2003. Prediction of mammalian microRNA targets. *Cell* 115, 787–798.
- Li, X., Bechara, R., Zhao, J., McGeachy, M.J., Gaffen, S.L., 2019. IL-17 receptor-based signaling and implications for disease. *Nat. Immunol.* 20, 1594–1602.



- Lim, G.P., Yang, F., Chu, T., Chen, P., Beech, W., Teter, B., Tran, T., Ubeda, O., Ashe, K. H., Frautschy, S.A., Cole, G.M., 2000. Ibuprofen suppresses plaque pathology and inflammation in a mouse model for Alzheimer's disease. *J. Neurosci.* 20, 5709–5714.
- Lokau, J., Nitz, R., Agthe, M., Monhasery, N., Aparicio-Siegmund, S., Schumacher, N., Wolf, J., Möller-Hackbarth, K., Waetzig, G.H., Grötzinger, J., Müller-Newen, G., Rose-John, S., Scheller, J., Garbers, C., 2016. Proteolytic cleavage governs interleukin-11 trans-signaling. *Cell Rep.* 14, 1761–1773.
- Luarde, A., Cisternas, P., Caviedes, A., Batiz, L.F., Lafourcade, C., Wyneken, U., Henzi, R., 2017. Astrocytes at the hub of the stress response: potential modulation of neurogenesis by miRNAs in astrocyte-derived exosomes. *Stem Cell. Int.* 2017, 1719050–1719050.
- Luo, Z.F., Jiang, X.H., Liu, H., He, L.Y., Luo, X., Chen, F.C., Tan, Y.L., 2021. miR-23b attenuates LPS-induced inflammatory responses in acute lung injury via inhibition of HDAC2. *Biochem. Genet.* 59, 604–616.
- Márquez Loza, A., Elias, V., Wong, C.P., Ho, E., Bermudez, M., Magnusson, K.R., 2017. Effects of ibuprofen on cognition and NMDA receptor subunit expression across aging. *Neuroscience* 344, 276–292.
- Morel, L., Chiang, M.S.R., Higashimori, H., Shoneye, T., Iyer, L.K., Yelick, J., Tai, A., Yang, Y., 2017. Molecular and functional properties of regional astrocytes in the adult brain. *J. Neurosci.* 37, 8706–8717.
- Nejad, C., Stunden, H.J., Gantier, M.P., 2018. A guide to miRNAs in inflammation and innate immune responses. *FEBS J.* 285, 3695–3716.
- Ouyang, Y.B., Xu, L., Yue, S., Liu, S., Giffard, R.G., 2014. Neuroprotection by astrocytes in brain ischemia: importance of microRNAs. *Neurosci. Lett.* 565, 53–58.
- Parepally, J.M., Mandula, H., Smith, Q.R., 2006. Brain uptake of nonsteroidal anti-inflammatory drugs: ibuprofen, flurbiprofen, and indomethacin. *Pharm. Res. (N. Y.)* 23, 873–881.
- Peng, J., Wu, S., Guo, C., Guo, K., Zhang, W., Liu, R., Li, J., Hu, Z., 2019. Effect of ibuprofen on autophagy of astrocytes during pentylenetetrazol-induced epilepsy and its significance: an experimental study. *Neurochem. Res.* 44, 2566–2576.
- Perini, G., Cotta Ramusino, M., Sinfioriani, E., Bernini, S., Petrachi, R., Costa, A., 2019. Cognitive impairment in depression: recent advances and novel treatments. *Neuropsychiatric Dis. Treat.* 15, 1249–1258.
- Pizzagalli, D.A., Holmes, A.J., Dillon, D.G., Goetz, E.L., Birk, J.L., Bogdan, R., Dougherty, D.D., Iosifescu, D.V., Rauch, S.L., Fava, M., 2009. Reduced caudate and nucleus accumbens response to rewards in unmedicated individuals with major depressive disorder. *Am. J. Psychiatr.* 166, 702–710.
- Rogers, J.T., Liu, C.C., Zhao, N., Wang, J., Putzke, T., Yang, L., Shinohara, M., Fryer, J.D., Kanekiyo, T., Bu, G., 2017. Subacute ibuprofen treatment rescues the synaptic and cognitive deficits in advanced-aged mice. *Neurobiol. Aging* 53, 112–121.
- Sayin, N., 2013. Inhibitory effects of acetylsalicylic acid and ibuprofen on interleukin-17 production. *Turkish Journal of Immunology* 1, 42–46.
- Shang, J.L., Cheng, Q., Yang, W.F., Zhang, M., Cui, Y., Wang, Y.F., 2014. Possible roles of COX-1 in learning and memory impairment induced by traumatic brain injury in mice. *Braz. J. Med. Biol. Res.* 47, 1050–1056.
- Smirnova, L., Gräfe, A., Seiler, A., Schumacher, S., Nitsch, R., Wulczyn, F.G., 2005. Regulation of miRNA expression during neural cell specification. *Eur. J. Neurosci.* 21, 1469–1477.
- Sofroniew, M.V., 2015. Astrocyte barriers to neurotoxic inflammation. *Nat. Rev. Neurosci.* 16, 249–263.
- Sofroniew, M.V., Vinters, H.V., 2010. Astrocytes: biology and pathology. *Acta Neuropathol.* 119, 7–35.
- Stellwagen, D., Malenka, R.C., 2006. Synaptic scaling mediated by glial TNF- $\alpha$ . *Nature* 440, 1054–1059.
- Sterpenich, V., Vidal, S., Hofmeister, J., Michalopoulos, G., Bancila, V., Warrot, D., Dayer, A., Desseilles, M., Aubry, J.M., Kosel, M., Schwartz, S., Vutsits, L., 2019. Increased reactivity of the mesolimbic reward system after ketamine injection in patients with treatment-resistant major depressive disorder. *Anesthesiology* 130, 923–935.
- Sun, F., Zhang, Y., Li, Q., 2017. Therapeutic mechanisms of ibuprofen, prednisone and betamethasone in osteoarthritis. *Mol. Med. Rep.* 15, 981–987.
- Takamura, M., Okamoto, Y., Okada, G., Toki, S., Yamamoto, T., Ichikawa, N., Mori, A., Minagawa, H., Takaishi, Y., Fujii, Y., Kaichi, Y., Akiyama, Y., Awai, K., Yamawaki, S., 2017. Patients with major depressive disorder exhibit reduced reward size coding in the striatum. *Prog. Neuro Psychopharmacol. Biol. Psychiatr.* 79, 317–323.
- Treadway, M.T., Admon, R., Arulpragasam, A.R., Mehta, M., Douglas, S., Vitaliano, G., Olson, D.P., Cooper, J.A., Pizzagalli, D.A., 2017. Association between interleukin-6 and striatal prediction-error signals following acute stress in healthy female participants. *Biol. Psychiatr.* 82, 570–577.
- Van Deun, J., Mestdagh, P., Agostinis, P., Akay, Ö., Anand, S., Anckaert, J., Martinez, Z. A., Baetens, T., Beghein, E., Bertier, L., Bex, G., Boere, J., Boukouris, S., Bremer, M., Buschmann, D., Byrd, J.B., Casert, C., Cheng, L., Cmoach, A., Daveloose, D., De Smedt, E., Demirsoy, S., Depoorter, V., Dhondt, B., Driedonks, T.A., Dudek, A., Elsharawy, A., Floris, I., Foers, A.D., Gärtner, K., Garg, A.D., Geuricx, E., Gettemans, J., Ghazavi, F., Giebel, B., Kormelink, T.G., Hancock, G., Helmsmoortel, H., Hill, A.F., Hyenne, V., Kalra, H., Kim, D., Kowal, J., Kraemer, S., Leidinger, P., Leonelli, C., Liang, Y., Lippens, L., Liu, S., Lo Cicero, A., Martin, S., Mathivanan, S., Mathiyalagan, P., Matussek, T., Milani, G., Monguió-Tortajada, M., Mus, L.M., Muth, D.C., Németh, A., Nolte-'t Hoen, E.N., O'Driscoll, L., Palmulli, R., Pfaffl, M.W., Primdall-Bengtson, B., Romano, E., Rousseau, Q., Sahoo, S., Sampaio, N., Samuel, M., Scicluna, B., Soen, B., Steels, A., Swinnen, J.V., Takatalo, M., Thamy, S., Théry, C., Tulkens, J., Van Audenhove, I., van der Grein, S., Van Goethem, A., van Herwijnen, M.J., Van Niel, G., Van Roy, N., Van Vliet, A.R., Vandamme, N., Vanhauwaert, S., Vergauwen, G., Verweij, F., Wallaert, A., Wauben, M., Witwer, K. W., Zonneveld, M.I., De Wever, O., Vandesompele, J., Hendrix, A., 2017. EV-TRACK: transparent reporting and centralizing knowledge in extracellular vesicle research. *Nat. Methods* 14, 228–232.
- Varcianna, A., Myszczyńska, M.A., Castelli, L.M., O'Neill, B., Kim, Y., Talbot, J., Nyberg, S., Nyamali, I., Heath, P.R., Stopford, M.J., Hautbergue, G.M., Ferraiuolo, L., 2019. Micro-RNAs secreted through astrocyte-derived extracellular vesicles cause neuronal network degeneration in C9orf72 ALS. *EBioMedicine* 40, 626–635.
- Vinckier, F., Gourion, D., Mouchabac, S., 2017. Anhedonia predicts poor psychosocial functioning: results from a large cohort of patients treated for major depressive disorder by general practitioners. *Eur. Psychiatr.* 44, 1–8.
- Wilson, R.P., Colizzi, M., Bossong, M.G., Allen, P., Kempton, M., Mtac Bhattacharyya, S., 2018. The neural substrate of reward anticipation in health: a meta-analysis of fMRI findings in the monetary incentive delay task. *Neuropsychol. Rev.* 28, 496–506.
- Wixey, J.A., Sukumar, K.R., Pretorius, R., Lee, K.M., Colditz, P.B., Bjorkman, S.T., Chand, K.K., 2019. Ibuprofen treatment reduces the neuroinflammatory response and associated neuronal and white matter impairment in the growth restricted newborn. *Front. Physiol.* 10.
- Yin, L., Xu, X., Chen, G., Mehta, N.D., Haroon, E., Miller, A.H., Luo, Y., Li, Z., Felger, J.C., 2019. Inflammation and decreased functional connectivity in a widely-distributed network in depression: centralized effects in the ventral medial prefrontal cortex. *Brain Behav. Immun.* 80, 657–666.
- Zhang, W., Lu, F., Xie, Y., Lin, Y., Zhao, T., Tao, S., Lai, Z., Wei, N., Yang, R., Shao, Y., He, J., 2019. miR-23b negatively regulates sepsis-induced inflammatory responses by targeting ADAM10 in human THP-1 monocytes. *Mediat. Inflamm.* 2019, 5306541.
- Zhao, Y., Mudge, M.C., Soll, J.M., Rodrigues, R.B., Byrum, A.K., Schwarzkopf, E.A., Bradstreet, T.R., Gygi, S.P., Edelson, B.T., Mosammaparast, N., 2018. OTUD4 is a phospho-activated K63 deubiquitinase that regulates MyD88-dependent signaling. *Mol. Cell* 69, 505–516 e505.
- Zhu, S., Pan, W., Song, X., Liu, Y., Shao, X., Tang, Y., Liang, D., He, D., Wang, H., Liu, W., Shi, Y., Harley, J.B., Shen, N., Qian, Y., 2012. The microRNA miR-23b suppresses IL-17-associated autoimmune inflammation by targeting TAB2, TAB3 and IKK- $\alpha$ . *Nat. Med.* 18, 1077–1086.
- Zidar, N., Odar, K., Glavac, D., Jerse, M., Zupanc, T., Stajer, D., 2009. Cyclooxygenase in normal human tissues – is COX-1 really a constitutive isoform, and COX-2 an inducible isoform? *J. Cell Mol. Med.* 13, 3753–3763.